Bioorganic Chemistry 84 (2019) 192–201

Contents lists available at ScienceDirect

Bioorganic Chemistry

journal homepage: www.elsevier.com/locate/bioorg

Ebsulfur as a potent scaffold for inhibition and labelling of New Delhi metallo-β-lactamase-1 *in vitro* and *in vivo*

Jianpeng Su[a], Jiayun Liu[b], Cheng Chen[a], Yuejuan Zhang[a], Kewu Yang[a,*]

[a] Key Laboratory of Synthetic and Natural Functional Molecule Chemistry of Ministry of Education, Chemical Biology Innovation Laboratory, College of Chemistry and Materials Science, Northwest University, 1 Xuefu Avenue, Xi'an 710127, PR China
[b] Department of Clinical Laboratory, Xijing Hospital, Air Force Medical University, Xi'an 710032, PR China

ARTICLE INFO

Keywords:
Antibiotic resistance
Metallo-β-lactamase
NDM-1
Inhibitor
Ebsulfurs

ABSTRACT

The superbug infection caused by New Delhi metallo-β-lactamase (NDM-1) has grown into an emerging threat, labelling and inhibition of NDM-1 has proven challenging due to its shuttling between pathogenic bacteria. Here, we report a potent covalent scaffold, ebsulfur, for targeting the protein *in vitro* and *in vivo*. Enzymatic kinetic study indicated that eighteen ebsulfurs gained except **1a–b** and **1f** inhibited NDM-1, exhibiting an IC_{50} value ranging of 0.16–9 μM, and **1g** was found to be the best, dose- and time-dependent inhibitor with an IC_{50} of 0.16 μM. Also, these ebsulfurs effectively restored the antibacterial activity of cefazolin against *E. coli* expressing NDM-1, and the best effect was observed to be from **1g**, **1i** and **1n**, resulting in an 256-fold reduction in MIC of the antibiotic at a dose of 16 μg/mL. The equilibrium dialysis study implied that the ebsulfur disrupted the coordination of one Zn(II) ion at active site of NDM-1. Labelling of NDM-1 using a constructed fluorescent ebsulfur **Ebs-R** suggested that the inhibitor covalently bound to the target through SDS-PAGE analysis *in vitro*. Also, labelling NDM-1 in living *E. coli* cells with **Ebs-R** by confocal microscopic imaging showed the real-time distribution change process of intracellular recombinant protein NDM-1. Moreover, the cytotoxicity of these ebsulfurs against L929 mouse fibroblastic cells was tested, and their capability to restore antibacterial activity of antibiotic against clinical strains *E. coli* EC08 producing NDM-1 was determined. The ebsulfur scaffold proposed here is valuable for development of the covalent irreversible inhibitors of NDM-1, and also for labelling the target *in vitro* and *in vivo*.

1. Introduction

β-Lactam antibiotics, including penicillins, cephalosporins, and carbapenems, remain the most important and frequently used antimicrobial agents, constituting more than 50% of the antibiotics prescribed worldwide [1]. However, the immoderate use of β-lactams has resulted in a large number of bacteria that are resistant to most all antibiotics. Most commonly, bacteria become resistant to β-lactams by producing β-lactamases, which catalyze the cleavage of β-lactam rings of the antibiotics [2,3]. β-Lactamases have been categorized into four classes: A, B, C, and D, depending on their amino acid sequence homologies [4]. Classes A, C, and D are referred to as serine-β-lactamases (SβLs) which utilize an active site serine to hydrolyze the β-lactam ring *via* an enzyme-acyl intermediate [5]. The class B enzymes, also called metallo-β-lactamases (MβLs), use either 1 or 2 Zn(II) ions to catalyze β-lactams hydrolysis [6]. MβLs are further divided into three subclasses B1, B2, and B3, based on their amino acid sequence and metal occupancies [1,7].

Antibiotic resistance has become a concerning global health problem. The development of β-lactamase inhibitors is an essential strategy for maintaining the usefulness of the existing β-lactam antibiotics. Although SβL inhibitors, such as clavulanic acid, tazobactam, and sulbactam, have been used clinically in combination with β-lactam antibiotics [1], there are no MβL inhibitors for clinic purpose to date [8]. Accordingly, the development of MβL inhibitor is urgently needed.

New Delhi metallo-β-lactamase-1 (NDM-1), a B1 subclass MβL, hydrolyzes almost all clinically available β-lactam antibiotics, including carbapenems which are considered "last resort antibiotics" [9–11]. The plasmid-encoded NDM-1 gene has been shown to horizontally transfer to other pathogenic bacteria and spread rapidly [12], therefore it is a daunting challenge to real-time monitor it in the dynamic cellular environment. Even worse, there is no simple and practical method for

* Corresponding author.
E-mail address: kwyang@nwu.edu.cn (K. Yang).

https://doi.org/10.1016/j.bioorg.2018.11.035
Received 16 September 2018; Received in revised form 19 November 2018; Accepted 20 November 2018
Available online 22 November 2018

labelling/tracking NDM-1 *in vitro* and *in vivo*.

Given the enormous clinical importance of NDM-1, a large number of NDM-1 inhibitors have been reported, such as D- and L-captopril [13,14], aspergillomarasmine A (AMA) [15], pyridine-2-carboxylic acid and its derivatives [16,17], and cyclic boronates [18]. Recently, ebselen was reported to be a covalent inhibitor of NDM-1 by forming a S—Se bond with the Cys221 residue at active site of the enzyme [19,20]. The crystal structures of NDM-1 have revealed the Zn(II) ion at the Zn_1 site is coordinated by His116, His118, His196, and a bridging water/hydroxide molecule (Wat1), while the Zn(II) ion at the Zn_2 site is coordinated by Asp120, Cys221, His263, the bridging water and an apical water molecule (Wat2) in NDM-1 [21]. Based on the residue Cys221 at active site of NDM-1, which was expected to be bound by the sulfur-containing molecules through forming disulfide bond in inhibiting the enzyme as proposed in Fig. 1, in this work, we developed a series of ebsulfur derivatives as previously reported methods [22–25], and also constructed a fluorescent labelling agent **Ebs-R** through attaching rhodamine B to an ebsulfur moiety, which was shown to label and visualize NDM-1 *in vitro* and *in vivo*. Moreover, the cytotoxicity of these ebsulfurs against L929 mouse fibroblastic cells was tested, and their capability to restore antibacterial activity of antibiotic against *E. coli* cells producing NDM-1 was determined.

2. Results and discussion

2.1. Chemistry

Eighteen ebsulfurs **1a–o**, **2a–c** and a fluorescent inhibitor **Ebs-R** were synthesized by a synthetic route as shown in Scheme S1 as previously reported methods [24,25]. Briefly, 2,2′-disulfanediyldibenzoic acid (**a**) react with $SOCl_2$ by refluxing in $SOCl_2$ to give 2,2′-disulfanediyldibenzoyl chloride (**b**) in a 80% yield, and **b** was treated with the corresponding aniline and Et_3N in DCM to afford compounds **1a–o** in 45–81% yield [25]. The intermediate isocyanates (**d**) was obtained by reaction of primary amine (**c**), triphosgene and Et_3N, and **d** reacted with **1a** to offer desire compounds **2a–c** [24]. Fluorescent inhibitor **Ebs-R** was synthesized by esterification of **1f** with Rhodamine B. The structures of ebsulfurs and **Ebs-R** are shown in Fig. 1. All compounds synthesized were characterized by ^1H and ^{13}C NMR and confirmed by HRMS (see Supporting Information).

2.2. Activity evaluation of ebsulfur on NDM-1 in vitro

To test whether these ebsulfurs were NDM-1 inhibitors, NDM-1 was over-expressed and purified as previously described [26], and detailed

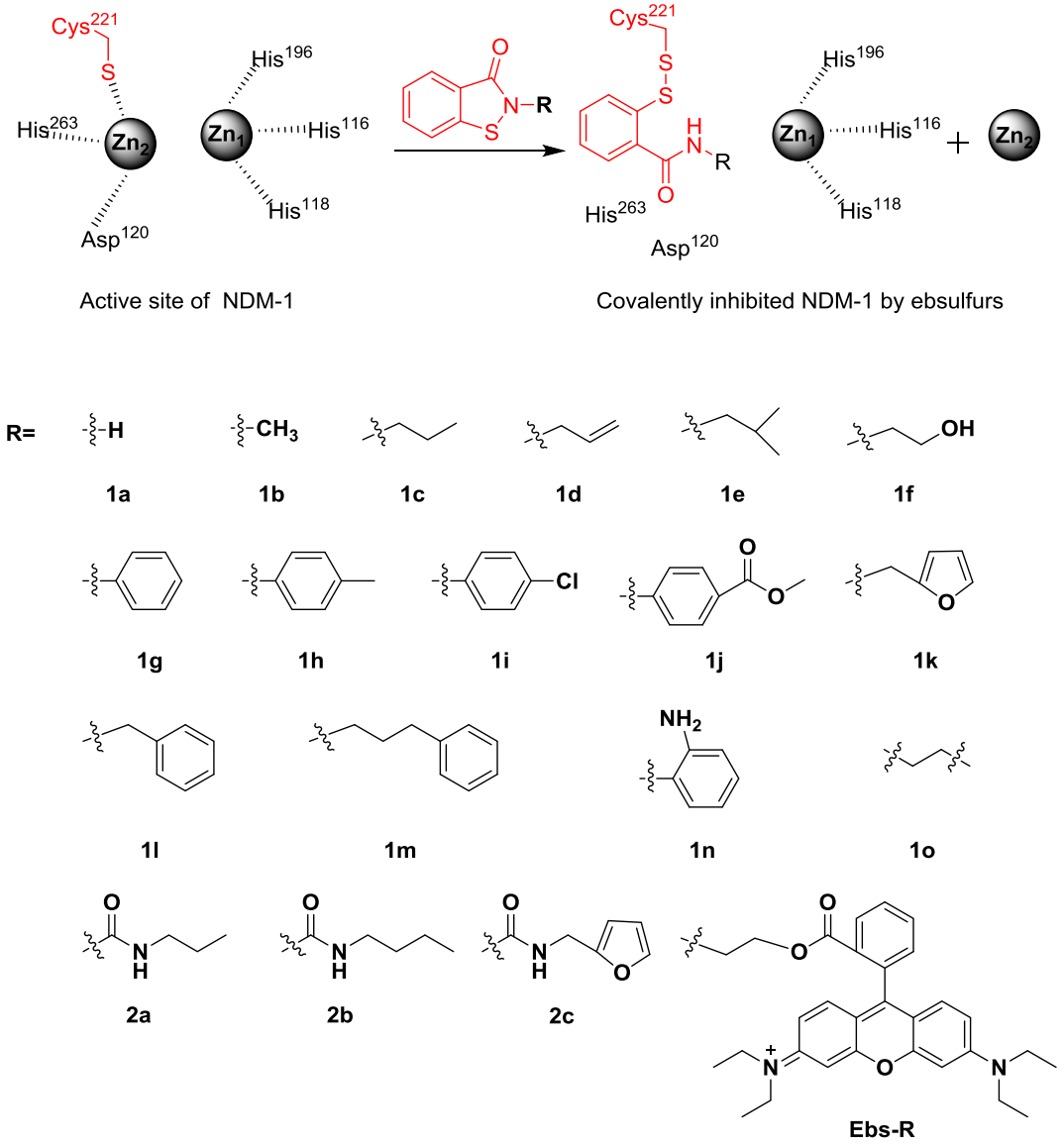

Fig. 1. The active site structures and proposed interaction mechanism of NDM-1 and the synthesized ebsulfurs with various substitutes.

Table 1
IC_{50} values of ebsulfurs against metallo-β-lactamases NDM-1.[a]

Compd	IC_{50} (μM)	Compd	IC_{50} (μM)
1a	98.6 ± 0.02	**1k**	0.79 ± 0.04
1b	24.1 ± 0.04	**1l**	0.77 ± 0.05
1c	8.17 ± 0.02	**1m**	1.05 ± 0.04
1d	2.5 ± 0.03	**1n**	0.66 ± 0.02
1e	2.32 ± 0.02	**1o**	0.2 ± 0.02
1f	85.3 ± 0.03	**2a**	0.26 ± 0.03
1g	0.16 ± 0.02	**2b**	0.72 ± 0.02
1h	0.48 ± 0.03	**2c**	0.4 ± 0.04
1i	0.59 ± 0.01	**Ebs-R**	0.74 ± 0.02
1j	0.52 ± 0.01		

[a] The substrate used was cefazolin and inhibitor concentration was varied between 0.1 and 100 μM.

in the Section 4. The enzyme inhibition experiments with these compounds were conducted on an Agilent UV8453 UV–Vis spectrophotometer using 40 μM cefazolin as substrate, and the concentrations of inhibitors were varied between 0 and 100 μM. Enzyme and inhibitor were pre-incubated for 20 h before adding cefazolin, which was then monitored at 262 nm, to determine the initial reaction rate in the absence and presence of inhibitor in triplicate, and the average value was recorded.

Percent inhibition, defined as enzyme activity without inhibitor (100%) minus residual activity with 10 μM inhibitor, is showed in Fig. S1. It is observed that all of these ebsulfurs except **1a**, **1b** and **1f** exhibited more than 50% inhibition on NDM-1 at a concentration of 50 nM. Also, the inhibitor concentrations causing 50% decrease of enzyme activity (IC_{50}) were determined using cefazolin as substrate. The IC_{50} data (Table 1) indicated that all compounds except **1a** and **1f** inhibited NDM-1 with an IC_{50} value range from 0.16 to 24 μM, and **1g** was found to be the best inhibitor (IC_{50} = 0.16 μM), which is consistent with its high percent inhibition at a concentration of 10 μM (Fig. S1).

2.3. Irreversible and time-dependent inhibition

In order to identify the inhibition mode of ebsulfurs, the hydrolysis of cefazolin (80 μM) inhibited by **1g** was real-time monitored at 262 nm on an Agilent UV8453 spectrometer (Fig. 2A). The enzyme concentration was 50 nM, and the hydrolysis is monitored within 20 min. It is clearly observed that the cefazolin was completely hydrolyzed within 200 s in the absence of inhibitor, while the residual concentration of cefazolin increased gradually with the increase of **1g** dose. When the concentration of the inhibitor was 4 μM, only approximately twenty-five percent antibiotics was hydrolyzed, implying that **1g** is an irreversible inactivator of NDM-1. Also, we monitored the residual activity of NDM-1 after different term of pre-incubate with **1g** for 24 h (Fig. 2B). It shows the activity of NDM-1 gradually decreases with pre-incubate time, and its activity reached the lowest level after pre-incubate for about 20 h, indicating that the ebsulfur is time-dependent inhibitor.

2.4. Equilibrium dialysis

To further understand the interaction of ebsulfur and NDM-1, equilibrium dialysis studies were conducted [17]. The metal content of protein samples was determined by using an IRIS Advantage Inductively Coupled Plasma spectrometer with atomic emission spectroscopy detection (ICP-AES). The protein samples were diluted to 8 μM with 50 mM Tris, pH 7.5. A calibration curve with four standards and a correlation coefficient of greater than 0.999 was generated using Zn reference solutions from Fisher Scientific. The following emission wavelengths were chosen to ensure the lowest detection limits possible: Zn, 213.856 nm [26]. As expected, the Zn (II) ion content of NDM-1 was significantly reduced when incubated with different concentrations of **1g** (Fig. 2C), when the concentration of **1g** was 25 μM, about an equivalent Zn(II) ions were removed from NDM-1, while when the inhibitor concentration continues to increase, the Zn(II) ion content in enzyme did not decrease, revealing that one Zn(II) ion from active site of each NDM-1 molecule was removed by the ebsulfur. In contrast, the Zn (II) ions of NDM-1 were almost completely removed when incubated with 200 μM EDTA. These results are consistent with the interaction mechanism of NDM-1 and ebsulfur that we proposed (Fig. 1).

2.5. MIC determination

The ability of ebsulfur to restore antimicrobial activity of cefazolin against *E. coli* producing NDM-1 was investigated by determining the minimum inhibitory concentrations (MICs) in the absence and presence of ebsulfurs **1a–o**, **2a–c** and **Ebs-R** as previously reported method [27]. *E. coli* BL21 (DE3) harboring plasmids pET26b-NDM-1 was used to assess these inhibitors. The MIC data (Table 2A) indicated that the ebsulfurs gradually increased antimicrobial effect of cefazolin against the *E. coli* cells with an increasing inhibitor dose, and the highest dose of **1g**, **1i** and **1n** tested (16 μg/mL) resulted in MICs of cefazolin 256-fold decreased, respectively. However, the inhibitors alone (16 μg/mL) did not inhibit cell growth, revealing that the efficacy of ebsulfurs to restore antibiotic activity is due to their inhibition to the NDM-1 harbored in bacteria. Further, to identify if ebsulfur exhibits activity against the bacteria expressing wild-type NDM-1, the capacity of ebsulfurs to restore the antimicrobial activity of cefazolin against clinical strain *E. coli* EC08 producing NDM-1 was investigated. The clinical strain was from the Health Science Center at Xi'an Jiaotong University (Xian, China). The MIC data (Table 2B) show that **1g–I, 1k, 1n** and **2a–b** resulted in 2–32-fold reduction in MIC of cefazolin, revealing that ebsulfur also restored activity of the antibiotic against clinical isolates producing NDM-1.

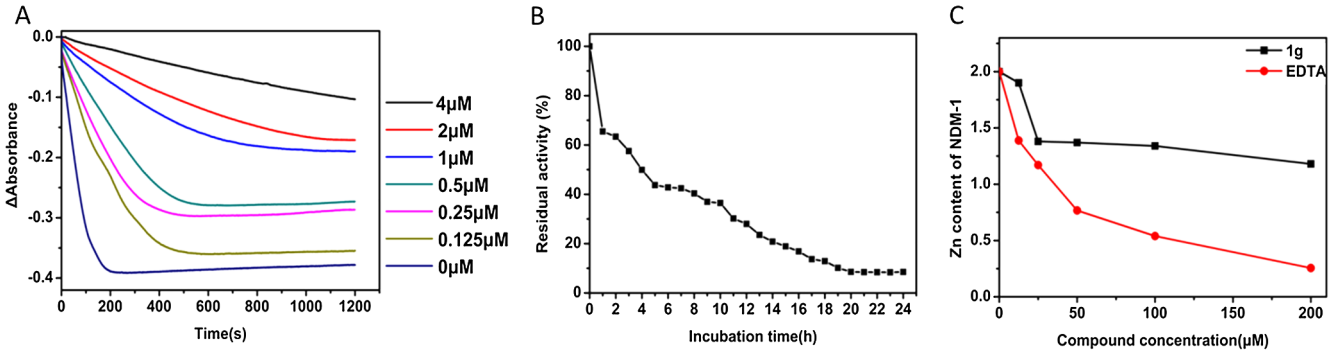

Fig. 2. Inhibition of cefazolin hydrolysis in the presence of NDM-1 enzyme by ebsulfur **1g** at various concentrations (A), the residual activity of NDM-1 (50 nM) after different term of pre-incubation with 4 μM **1g** (B), and the metal content of NDM-1 (8 μM) after dialysis versus various concentrations of EDTA or **1g** in 50 mM HEPES, pH 7.5 (C).

Table 2
Antibacterial activities (MICs, μg/mL) of cefazolin against *E. coli* BL21 strain expressing NDM-1 in the absence and presence of ebsulfur at a concentration ranging from 2 to 16 μg/mL (A), and cefazolin against clinical strain *E. coli* EC08 producing NDM-1 in the absence and presence of ebsulfur at a concentration ranging from 16 to 128 μg/mL (B).

A

Compd\conc	cefazolin	+2	+4	+8	+16	Compd\conc	cefazolin	+2	+4	+8	+16
1a	256	256	256	128	128	**1k**	256	128	32	8	2
1b	256	256	128	128	64	**1l**	256	128	32	8	4
1c	256	256	128	64	64	**1m**	256	128	64	32	8
1d	256	128	64	32	16	**1n**	256	128	8	2	1
1e	256	128	64	16	16	**1o**	256	256	128	64	64
1f	256	256	256	128	64	**2a**	256	128	64	8	2
1g	256	64	8	4	1	**2b**	256	128	64	16	2
1h	256	128	8	8	2	**2c**	256	128	64	64	16
1i	256	64	32	8	1	**Ebs-R**	256	256	128	32	32
1j	256	256	64	16	4						

B

Compd\conc	cefazolin	+16	+32	+64	+128	Compd\conc	cefazolin	+16	+32	+64	+128
1g	10,000	10,000	5000	5000	625	**1n**	10,000	5000	5000	1250	312.5
1h	10,000	10,000	10,000	5000	5000	**2a**	10,000	10,000	10,000	5000	5000
1i	10,000	10,000	5000	5000	1250	**2b**	10,000	10,000	10,000	10,000	5000
1k	10,000	10,000	5000	1250	1250						

2.6. Real-time activity monitoring of NDM-1 in living E. coli cells

A simple and straightforward UV–Vis approach was employed for real-time activity monitoring of NDM-1 in living bacterial cells in the presence and absence of **1g** [28]. *E. coli* BL21 cells that produce NDM-1 were used to assess the ebsulfur inhibitor. Inhibition of cefazolin hydrolysis in *E. coli* cells harboring NDM-1 by ebsulfur **1g** is shown in Fig. 3A. It is clearly observed that **1g** effectively inhibits NDM-1 in living cells, exhibiting an IC_{50} value of 35.1 μM on the cells (Fig. 3B), which is much larger than the data (0.16 μM) from above assays *in vitro* using the same antibiotic as enzyme substrate. This is probably due to the poor transport through porin or efflux pump, which limits the inhibitor's access to NDM-1 in the native environment of bacteria and consequently results in reduced inhibition of cefazolin hydrolysis [28].

2.7. Fluorescent labelling NDM-1 with Ebs-R

To identify whether the binding of ebsulfurs to NDM-1 occurred, we constructed a fluorescent ebsulfur **Ebs-R** by introducing Rhodamine B onto ebsulfur molecule and identified the binding of protein-small molecule by SDS-PAGE. The scheme of labelling NDM-1 with **Ebs-R** is illustrated in Fig. 4A. The purified NDM-1 was incubated with **Ebs-R** and the resulting sample was assessed by SDS-PAGE. The labelled protein was observed by photographing with iPhone 6 s under UV illumination (365 nm) followed by staining with Coomassie Brilliant Blue (CBB). Comparison of the gel pictures gave an indication of protein labelling [29]. When NDM-1 sample was mixed with different concentrations of **Ebs-R**, a series of yellow protein bands with different fluorescence intensities were observed, and the CBB staining suggested that the bands are corresponded to NDM-1 (Fig. 4B, Lanes 6–11). In contrast, when NDM-1 was treated with Rhodamine B, no yellow protein bands were observed (Fig. 4B, Lane 3), indicating that the Rhodamine B could not label NDM-1. Besides, when adding 5% mercaptoethanol to the gel loading buffer, incubation of NDM-1 with **Ebs-R** did not result in a surveyable yellow band (Fig. 4B, Lane 4), implying that the disulfide bond formed between NDM-1 and **Ebs-R** was reduced by mercaptoethanol. Also, **Ebs-R** exhibited a dose- and time-dependent labelling to NDM-1 (Fig. 4B and 4C), which are consistent with those of

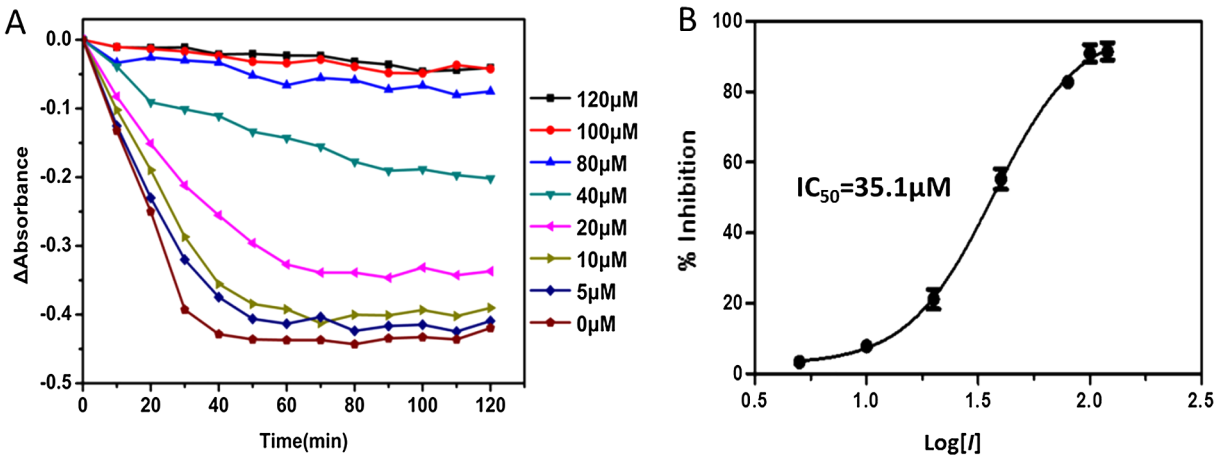

Fig. 3. Inhibition of cefazolin hydrolysis in NDM-1 harbored *E. coli* cells by **1g** at various concentrations (A), and IC_{50} measurement for *E. coli* BL21 cells (B). For each experiment, the *E. coli* cells harboring NDM-1 (OD_{600} = 0.2) were first incubated with **1g** for 10 min and 100 μM cefazolin was subsequently added.

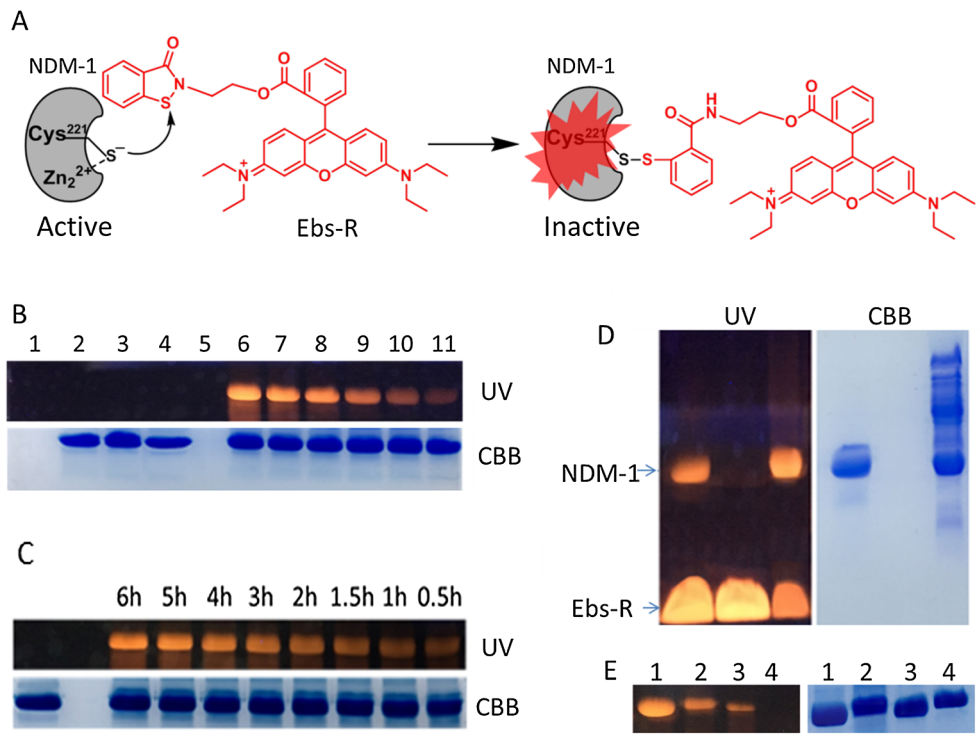

Fig. 4. The gel electrophoresis analysis of NDM-1-labelled by the fluorescent reagent **Ebs-R**. (A) Structure and mechanism of labelling NDM-1 with **Ebs-R.** (B) Lanes 1–3: 80 μM **Ebs-R**, 20 μM NDM-1, 20 μM NDM-1 treated with 80 μM Rhodamine B; Lane 4: 20 μM NDM-1 and 80 μM **Ebs-R**(containing 5% β-ME); Lanes 6–11: 20 μM NDM-1 was treated with different concentrations of **Ebs-R** (final concentrations were 80, 40, 20, 10, 5, 2.5 μM, respectively). (C) Lane 1: control, 20 μM NDM-1; Lanes 3–10: 20 μM NDM-1 and 20 μM **Ebs-R** incubated for different time. (D) Left Lane: 40 μM purified NDM-1 and 40 μM **Ebs-R**; middle Lane: 40 μM **Ebs-R**; right Lane: cell lysate was treated with 40 μM **Ebs-R**. (E) Lanes 1–4: 20 μM MβLs (from left to right: NDM-1, IMP-1, ImiS and L1) was treated with 20 μM **Ebs-R**.

the above irreversible and time-dependent inhibition studies. These characterizations suggested that **Ebs-R** covalently bound to the cysteine at active site of NDM-1.

In vivo experiments were also carried out with cells grown in the presence of **Ebs-R** (Fig. 4D). *E. coli* BL21 cells harboring NDM-1 (OD_{600} = 0.5) were incubated with 40 μM **Ebs-R** at 37 °C for 2 h, the cells were washed with PBS through centrifugation for five times (10,400*g*, 10 min) to remove any adsorbed **Ebs-R** on the cell surface, and then resuspended in PBS, lysed by ultrasonication and the resulting supernatant was analyzed by SDS-PAGE. It was clearly observed that **Ebs-R** can penetrate through the cell membrane and label the NDM-1 Inside cells. Also, to assay whether the ebsulfur selectively label MβLs, **Ebs-R** (20 μM) was employed for labelling the MβLs from B1-B3 subclasses. As shown in Fig. 4E, the NDM-1 and IMP-1 (B1) and ImiS (B2) were labelled by **Ebs-R** in varying degrees, but L1 was not, suggesting that the ebsulfur, like ebselen [20], targets the MβLs with cysteine residue at the active site(s), while the most prominent fluorescent band to NDM-1 suggesting that the ebsulfur could be for labelling the protein that is over-expressed *in vivo* [30].

2.8. Tracking NDM-1 and Real-time imaging in living bacterial cells with Ebs-R

To track the NDM-1 inside living bacterial cells, fluorescence imaging of the *E. coli* BL21 cells harboring NDM-1 with **Ebs-R** was performed using Andor Dragonfly Confocal Microscope (Andor, UK) [31]. Fig. 5 shows the images of NDM-1 *E. coli* cells incubated with **Ebs-R** in MHB for different time. The interaction of **Ebs-R** with bacteria was imaged using microscopy technique, where a clear visualization of the interation of ebsulfur and intracellular enzyme (NDM-1) has been intuitively demonstrated. **Ebs-R** was found to associate at certain sites on and in the bacteria depending on incubation time. Incubation with **Ebs-R** for 8 h, a high density of bacterial cells with either membrane-associated or uniform localization of inhibitor throughout the cytosol of the bacterial cells was observed (Fig. 5A). Incubation for 16 or 24 h, we observed that enzyme NDM-1 accumulated at the cell poles (Fig. 5B–C), possibly reflecting the formation of inclusion bodies [32]. Furthermore, incubation for 48 h, we observed that the enzyme finally looked like diffused probably due to the lysed of bacterial cells (Fig. 5D). The real-time distribution change process of intracellular recombinant protein NDM-1 is shown in Fig. 5E–H.

2.9. Uptake of ebsulfurs by bacterial cells

Flow cytometer would be more appreciate technique for measurement of fluorescence intensity of only those labelled inhibitors that are internalized into the cells [33]. NDM-1 *E. coli* cells were incubated with **Ebs-R** at concentration of 0, 10, 20 and 40 μM, respectively. After a certain period of incubation, the cells were repeatedly washed with PBS (to remove any **Ebs-R** adsorbed on the surface of cells) and investigated by analysis using flow cytometer. The results of cellular uptake of inhibitor into NDM-1 *E. coli* cells are shown in Fig. 6. It shows that the ratio of detectable labelled *E. coli* cells increase from 9.8 to 76.6% with the increase of **Ebs-R** dose from 10 to 40 μM, exhibiting a dose-dependent cellular uptake, in comparison with the controls, revealing that the ebsulfur molecules can bond stably with bacteria.

2.10. Cytotoxicity assay

For biomedical applications, the potential toxicity of ebsulfur inhibitors is a major concern. As the representatives of ebsulfurs, **1g**, **2a** and **Ebs-R** were subjected to a cytotoxicity assay using mouse fibroblast cells (L929) treated with different inhibitor concentrations (2.5, 5, 10, 20, 40, and 80 μM). As shown in Fig. 7, no compounds except **1g** tested affected viability of the L929 mouse fibroblastic cells at a concentration up to 40 μM, indicating that these compounds have low cytotoxicity and may be used clinical purposes.

3. Conclusion

Based on the residue Cys221 at active site of NDM-1, which was expected to be bound by the sulfur-containing molecules through forming a disulfide bond in inhibiting the enzyme as proposed in Fig. 1, eighteen ebsulfur derivatives were synthesized, characterized by ^{1}H, ^{13}C NMR and HRMS, and evaluated *in vitro* and in *in vivo*. All of these ebsulfurs gained inhibited NDM-1, especially **1g**, exhibiting an IC_{50}

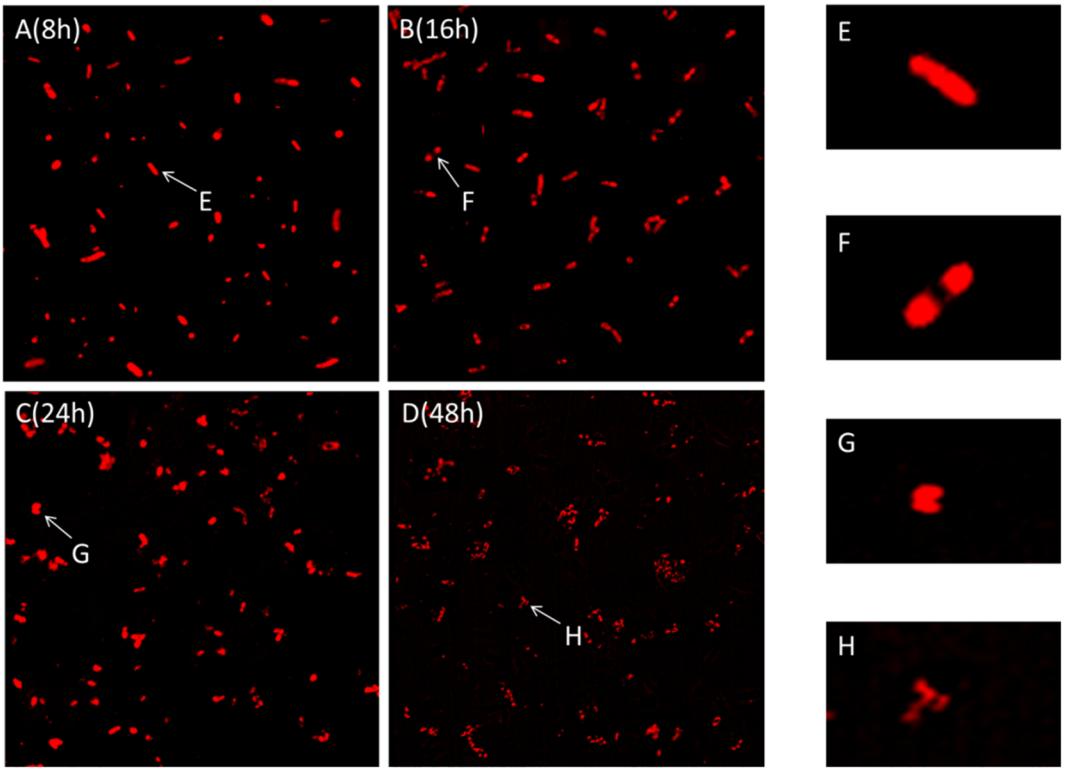

Fig. 5. Confocal microscopic real-time imaging of *E. coli* BL21 cells expressing NDM-1 after treated with **Ebs-R** (40 μM) for different time (A-D), and the real-time distribution change process of the recombinant protein NDM-1 inside living *E. coli* BL21 cells (E–H).

value of 0.16 μM. Also, these ebsulfurs effectively restored the antibacterial activities of cefazolin against *E. coli* expressing NDM-1, and the best effect was observed to be from **1g**, **1i** and **1n**, resulting in an 256-fold reduction in MIC of the antibiotic at a concentration of 16 μg/mL. Inhibitory and equilibrium dialysis studies suggested that the ebsulfur time-dependently and covalently binds to NDM-1, which has been examined with fluorescent **Ebs-R** constructed through SDS-PAGE analysis. Real-time activity monitoring of the NDM-1 inside living *E. coli* BL21 cells indicated that **1g** effectively inhibited the enzyme with an IC_{50} value of 35.1 μM. Tracking the NDM-1 in living *E. coli* cells

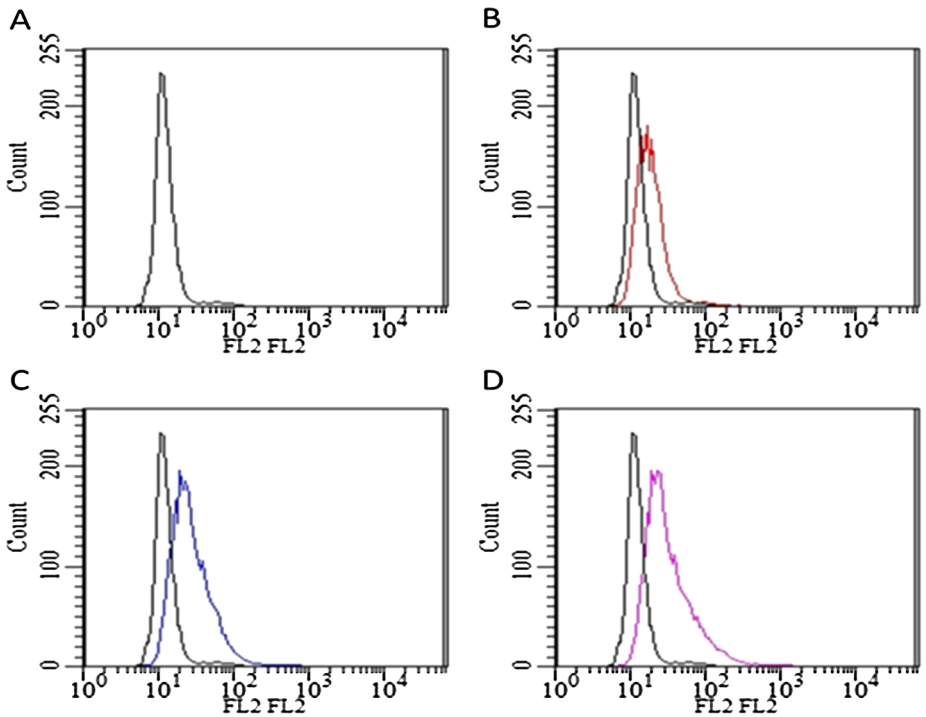

Fig. 6. Flow cytometer analysis of NDM-1 *E. coli* cells incubation with **Ebs-R** at different concentrations. NDM-1 *E. coli* cells were incubated with 0 (A), 10 (B), 20 (C), and 40 μM **Ebs-R** (D).

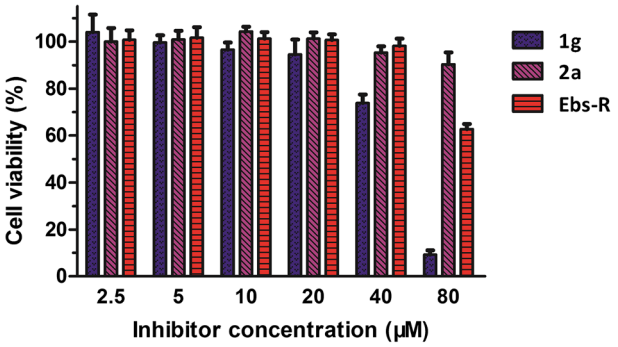

Fig. 7. Cytotoxicity assay of ebsulfurs **1g**, **2a** and **Ebs-R** on L929 cells at an inhibitor concentration ranging from 2.5 to 80 μM. DMSO was used as a negative control, and cell viability was measured by MTT assay.

through labelling it with **Ebs-R** by confocal microscopic imaging showed that the target initially distributed uniformly in the cytosol of bacteria cells, then accumulated in formation of inclusion bodies at the cell poles, and finally dispersed probably due to the lysed of bacterial cells. The ebsulfur scaffold proposed here is valuable for development of the covalent NDM-1 inhibitors and also for labelling the target *in vitro* and *in vivo*.

4. Experimental

4.1. Materials

The reagents were purchased from Aladdin (Shanghai) Trading Co., Ltd. All other starting materials were purchased from commercial sources and purified using standard methods. Analytical thin layer chromatography (TLC) was carried out on silica gel F254 plates with visualization by ultraviolet radiation. ^{1}H and ^{13}C NMR spectra were recorded on a Bruker 400 MHz NMR spectrometer. Chemical shifts are given in parts per million (ppm) on the delta scale. The peak patterns are reported as singlet (s), doublet (d), triplet (t), quartet (q), and multiplet (m). The spectra were recorded with TMS as internal standard. Coupling constants (*J*) were reported in Hertz (Hz). Mass spectra were obtained on a micro TOF-Q (BRUKER) mass spectrometer. Activity evaluation of inhibitors was performed on an Agilent 8453 UV–Vis spectrometer. Confocal fluorescence images were collected on an Andor Dragonfly Confocal Microscope (Andor, UK).

4.2. Chemistry

4.2.1. Preparation of ebsulfurs 1a–o following procedure A

2-(Chlorosulfanyl)benzoyl chloride (**b**) has been obtained by 2,2′-disulfanediyldibenzoic acid (**a**) react with $SOCl_2$ according to the procedure described [22]. To a stirred and ice-cooled mixture of primary amine (3 mmol) and Et_3N (0.45 mL, 3.2 mmol) in anhydrous CH_2Cl_2 (40 mL), 2, 2′-dithiobenzoyl chloride (**b**, 0.50 g, 1.5 mmol) in anhydrous CH_2Cl_2 (20 mL) was added dropwise over 20 min. The reaction mixture was warmed-up to RT, stirred for 12 h, and washed with aq. sat. $NaHCO_3$ (30 mL) and H_2O (30 mL). The organic layer was dried over anhydrous Na_2SO_4, concentrated in vacuo, and the resulting residue was purified by flash column chromatography (SiO_2, EtOAc:hexane/1:2) to afford the final compounds **1a–o** [25].

*4.2.1.1. 1,2-benzisothiazoline-3-one **(1a)***. Compound **1a** was prepared according to standard procedure A by using **b** and ammonia aqueous solution, obtained a white solid in 80% yield. ^{1}H NMR (400 MHz, $CDCl_3$) δ 8.16–8.08 (m, 1H), 7.74–7.65 (m, 2H), 7.52–7.44 (m, 1H). ^{13}C NMR (101 MHz, DMSO) δ 165.26, 147.86, 130.51, 125.31, 125.17, 124.59, 121.93. HRMS (ESI) *m/z*: 152.0167 (Calcd. for $[M+H^+]^+$: 152.0165 *m/z*).

*4.2.1.2. 2-methylbenzo[d]isothiazol-3(2H)-one **(1b)***. Compound **1b** was prepared according to standard procedure A by using **b** and Methylamine aqueous solution, obtained a white solid in 75% yield. ^{1}H NMR (400 MHz, $CDCl_3$) δ 8.02 (d, J = 7.9 Hz, 1H), 7.64–7.50 (m, 2H), 7.43–7.35 (m, 1H), 3.43 (s, 3H). ^{13}C NMR (101 MHz, $CDCl_3$) δ 165.52, 139.95, 131.70, 126.51, 125.47, 124.35, 120.25, 30.44. HRMS (ESI) *m/z*: 188.0132 (Calcd. for $[M+Na^+]^+$: 188.0141 *m/z*).

*4.2.1.3. 2-propylbenzo[d]isothiazol-3(2H)-one **(1c)***. Compound **1c** was prepared according to standard procedure A by using **b** and Propylamine, obtained a yellow solid in 60% yield. ^{1}H NMR (400 MHz, $CDCl_3$) δ 7.98 (d, J = 7.9 Hz, 1H), 7.52 (dt, J = 10.2, 4.3 Hz, 2H), 7.34 (ddd, J = 8.0, 6.7, 1.4 Hz, 1H), 3.88–3.76 (m, 2H), 1.82–1.67 (m, 2H), 0.98–0.89 (m, 3H). ^{13}C NMR (101 MHz, $CDCl_3$) δ 165.29, 140.12, 131.59, 126.50, 125.34, 124.73, 120.33, 45.44, 22.86, 11.10. HRMS (ESI) *m/z*: 194.0640 (Calcd. for $[M+H^+]^+$: 194.0634 *m/z*).

*4.2.1.4. 2-allylbenzo[d]isothiazol-3(2H)-one **(1d)***. Compound **1d** was prepared according to standard procedure A by using **b** and Allylamine, obtained a yellow solid in 66% yield. ^{1}H NMR (400 MHz, $CDCl_3$) δ 8.05 (d, J = 7.9 Hz, 1H), 7.66–7.51 (m, 2H), 7.40 (t, J = 7.4 Hz, 1H), 5.94 (ddt, J = 16.4, 10.1, 6.1 Hz, 1H), 5.40–5.26 (m, 2H), 4.51 (d, J = 6.1 Hz, 2H). ^{13}C NMR (101 MHz, $CDCl_3$) δ 165.15, 140.40, 132.36, 131.81, 126.74, 125.48, 124.67, 120.39, 119.32, 46.20. HRMS (ESI) *m/z*: 192.0470 (Calcd. for $[M+H^+]^+$: 192.0477 *m/z*).

*4.2.1.5. 2-isobutylbenzo[d]isothiazol-3(2H)-one **(1e)***. Compound **1e** was prepared according to standard procedure A by using **b** and isobutylamine, obtained a yellow solid in 65% yield. ^{1}H NMR (400 MHz, $CDCl_3$) δ 8.00 (d, J = 7.9 Hz, 1H), 7.55 (ddd, J = 14.1, 10.5, 4.4 Hz, 2H), 7.35 (ddd, J = 8.0, 6.9, 1.3 Hz, 1H), 3.68 (d, J = 7.4 Hz, 2H), 2.19–2.00 (m, 1H), 0.95 (d, J = 6.7 Hz, 6H). ^{13}C NMR (101 MHz, $CDCl_3$) δ 165.49, 140.18, 131.62, 126.59, 125.33, 124.61, 120.25, 51.09, 28.98, 19.87. HRMS (ESI) *m/z*: 230.0618 (Calcd. for $[M+Na^+]^+$: 230.0610 *m/z*).

*4.2.1.6. 2-(2-hydroxyethyl)benzo[d]isothiazol-3(2H)-one **(1f)***. Compound **1f** was prepared according to standard procedure A by using **b** and 2-Aminoethanol, obtained a yellow solid in 55% yield. ^{1}H NMR (400 MHz, $CDCl_3$) δ 8.08–7.99 (m, 1H), 7.62 (ddd, J = 8.2, 7.1, 1.2 Hz, 1H), 7.55 (d, J = 8.1 Hz, 1H), 7.41 (ddd, J = 8.0, 7.1, 1.0 Hz, 1H), 4.05 (dt, J = 6.4, 1.7 Hz, 2H), 4.01–3.93 (m, 2H). ^{13}C NMR (101 MHz, $CDCl_3$) δ 166.41, 140.72, 131.97, 126.63, 125.60, 124.22, 120.23, 62.00, 47.49. HRMS (ESI) *m/z*: 218.0239 (Calcd. for $[M+Na^+]^+$:218.0246 *m/z*).

*4.2.1.7. 2-phenylbenzo[d]isothiazol-3(2H)-one **(1g)***. Compound **1g** was prepared according to standard procedure A by using **b** and Aniline, obtained a yellow solid in 85% yield. ^{1}H NMR (400 MHz, DMSO) δ 8.06 (d, J = 8.1 Hz, 1H), 8.00–7.93 (m, 1H), 7.82–7.67 (m, 3H), 7.60–7.46 (m, 3H), 7.42–7.32 (m, 1H). ^{13}C NMR (101 MHz, DMSO) δ 163.75, 140.55, 137.64, 133.05, 129.92, 127.44, 126.64, 126.48, 124.91, 124.80, 122.40. HRMS (ESI) *m/z*: 228.0472 (Calcd. for $[M+H^+]^+$: 228.0477 *m/z*).

*4.2.1.8. 2-(p-tolyl)benzo[d]isothiazol-3(2H)-one **(1h)***. Compound **1h** was prepared according to standard procedure A by using **b** and p-Toluidine, obtained a yellow solid in 83% yield. ^{1}H NMR (400 MHz, $CDCl_3$) δ 8.09 (d, J = 7.9 Hz, 1H), 7.64 (ddd, J = 8.2, 7.2, 1.2 Hz, 1H), 7.59–7.51 (m, 3H), 7.47–7.39 (m, 1H), 7.31–7.21 (m, 2H), 2.38 (s, 3H). ^{13}C NMR (101 MHz, $CDCl_3$) δ 164.07, 139.95, 137.23, 134.52, 132.25, 129.97, 127.12, 125.76, 124.83, 124.75, 120.13, 21.17. HRMS (ESI) *m/z*: 242.0645(Calcd. for $[M+H^+]^+$: 242.0634 *m/z*).

4.2.1.9. 2-(4-chlorophenyl)benzo[d]isothiazol-3(2H)-one ***(1i)***. Compound **1i** was prepared according to standard procedure A by using **b** and p-Chlorophenylamine, obtained a yellow solid in 82% yield. ^{1}H NMR (400 MHz, $CDCl_3$) δ 8.10 (d, J = 7.9 Hz, 1H), 7.73–7.64 (m, 3H), 7.59 (d, J = 8.1 Hz, 1H), 7.51–7.39 (m, 3H). ^{13}C NMR (101 MHz, $CDCl_3$) δ 164.13, 139.64, 135.82, 132.61, 132.52, 129.49, 127.28, 126.01, 125.65, 124.60, 120.14. HRMS (ESI) *m/z*: 283.9899 (Calcd. for $[M+Na^+]^+$: 283.9907 *m/z*).

4.2.1.10. Methyl 4-(3-oxobenzo[d]isothiazol-2(3H)-yl)benzoate ***(1j)***. Compound **1j** was prepared according to standard procedure A by using **b** and 4-aminobenzoic acid methyl ester, obtained a yellow solid in 78% yield. ^{1}H NMR (400 MHz, $CDCl_3$) δ 8.19–8.07 (m, 3H), 7.93–7.85 (m, 2H), 7.68 (dd, J = 7.1, 1.1 Hz, 1H), 7.60 (d, J = 8.1 Hz, 1H), 7.50–7.42 (m, 1H), 3.94 (s, 3H). ^{13}C NMR (101 MHz, $CDCl_3$) δ 166.28, 164.18, 141.65, 139.47, 132.85, 130.85, 127.78, 127.37, 126.09, 124.84, 122.90, 120.13, 52.27. HRMS (ESI) *m/z*: 308.0349 (Calcd. for $[M+Na^+]^+$: 308.0351 *m/z*).

4.2.1.11. 2-(furan-2-ylmethyl)benzo[d]isothiazol-3(2H)-one ***(1k)***. Compound **1k** was prepared according to standard procedure A by using **b** and furan-2-ylmethanamine, obtained a yellow solid in 75% yield. ^{1}H NMR (400 MHz, $CDCl_3$) δ 8.10–8.01 (m, 1H), 7.59 (ddd, J = 8.3, 7.1, 1.2 Hz, 1H), 7.54–7.48 (m, 1H), 7.45–7.34 (m, 2H), 6.43 (dd, J = 3.2, 0.5 Hz, 1H), 6.37 (dd, J = 3.2, 1.9 Hz, 1H), 5.06 (s, 2H). ^{13}C NMR (101 MHz, $CDCl_3$) δ 165.07, 149.28, 143.20, 140.46, 131.93, 126.83, 125.51, 124.42, 120.39, 110.64, 109.82, 40.08. HRMS (ESI) *m/z*: 232.0418 (Calcd. for $[M+H^+]^+$: 232.0426 *m/z*).

4.2.1.12. 2-benzylbenzo[d]isothiazol-3(2H)-one ***(1l)***. Compound **1l** was prepared according to standard procedure A by using **b** and Benzylamine, obtained a yellow solid in 50% yield. ^{1}H NMR (400 MHz, DMSO) δ 7.93 (dd, J = 13.5, 8.0 Hz, 2H), 7.73–7.65 (m, 1H), 7.46 (t, J = 7.5 Hz, 1H), 7.41–7.27 (m, 5H), 5.03 (s, 2H). ^{13}C NMR (101 MHz, DMSO) δ 164.86, 141.03, 137.40, 132.42, 129.17, 128.40, 126.15, 122.47, 46.79. HRMS (ESI) *m/z*: 264.0458 (Calcd. for $[M+Na^+]^+$: 264.0459 *m/z*).

4.2.1.13. 2-(3-phenylpropyl)benzo[d]isothiazol-3(2H)-one ***(1m)***. Compound **1m** was prepared according to standard procedure A by using **b** and 3-phenylpropan-1-amine, obtained a yellow solid in 52% yield. ^{1}H NMR (400 MHz, $CDCl_3$) δ 8.09 (d, J = 7.8 Hz, 1H), 7.70–7.55 (m, 2H), 7.44 (t, J = 7.2 Hz, 1H), 7.34 (t, J = 7.4 Hz, 2H), 7.30–7.20 (m, 3H), 3.98 (t, J = 7.0 Hz, 2H), 2.75 (t, J = 7.7 Hz, 2H), 2.21–2.07 (m, 2H). ^{13}C NMR (101 MHz, $CDCl_3$) δ 165.40, 140.92, 140.14, 131.74, 128.50, 128.42, 126.63, 126.13, 125.50, 124.74, 120.39, 43.49, 32.80, 31.18. HRMS (ESI) *m/z*: 270.0955 (Calcd. for $[M+H^+]^+$: 270.0953 *m/z*).

4.2.1.14. 2-(2-aminophenyl)benzo[d]isothiazol-3(2H)-one ***(1n)***. Compound **1n** was prepared according to standard procedure A by using **b** and 1,2-diaminobenzene, obtained a yellow solid in 56% yield. ^{1}H NMR (400 MHz, DMSO) δ 8.06–7.98 (m, 1H), 7.98–7.88 (m, 1H), 7.80–7.69 (m, 1H), 7.58–7.44 (m, 1H), 7.24–7.09 (m, 2H), 6.92–6.80 (m, 1H), 6.72–6.58 (m, 1H), 5.24 (s, 2H). ^{13}C NMR (101 MHz, DMSO) δ 164.25, 146.59, 142.21, 132.41, 130.27, 130.11, 126.53, 125.89, 124.61, 122.32, 120.74, 116.56. HRMS (ESI) *m/z*: 243.0579 (Calcd. for $[M+H^+]^+$: 243.0586 *m/z*).

4.2.1.15. 2,2′-(ethane-1,2-diyl)bis(benzo[d]isothiazol-3(2H)-one) ***(1o)***. Compound **1o** was prepared according to standard procedure A by using **b** and ethylenediamine, obtained a yellow solid in 75% yield. ^{1}H NMR (400 MHz, DMSO) δ 7.93 (d, J = 8.1 Hz, 2H), 7.84 (d, J = 7.8 Hz, 2H), 7.66 (dd, J = 11.2, 4.0 Hz, 2H), 7.42 (t, J = 7.4 Hz, 2H), 4.16 (s, 4H). ^{13}C NMR (101 MHz, DMSO) δ 165.10, 141.37, 132.33, 126.10, 125.96, 124.23, 122.47, 42.94. HRMS (ESI) *m/z*: 351.0225 (Calcd. for $[M+Na^+]^+$: 351.0232 *m/z*).

4.2.2. Preparation of ebsulfurs 2a–c following procedure B

To a solution of triphosgene (2.96 g, 10 mmol) in DCM (20 mL) was added dropwise to primary amine **c** (10 mmol) in DCM (20 mL) followed by dropwise addition of triethylamine (3 mL) in DCM (10 mL). The solvent was removed on a rotary evaporator. The resulting residue (**d**) was dissolved in DCM (20 mL), and **1a** (1.51 g, 10 mmol) in THF (20 mL) was added. After the mixture was refluxed for 30 min, the solvent was removed on a rotary evaporator, the residue was dissolved in acetone (30 mL) and mixed with water (30 mL), the resulting precipitate was collected on a funnel by vacuum filtration and washed with water–acetone (1:1, 4 × 5 mL) to afford the final compounds **2a–c** [24].

4.2.2.1. 3-oxo-N-propylbenzo[d]isothiazole-2(3H)-carboxamide ***(2a)***. Compound **2a** was prepared according to standard procedure B by using **1a** and Propylamine, obtained a white solid in 76% yield. ^{1}H NMR (400 MHz, $CDCl_3$) δ 8.90 (s, 1H), 8.02 (d, J = 7.9 Hz, 1H), 7.77–7.64 (m, 1H), 7.58 (d, J = 8.1 Hz, 1H), 7.49–7.36 (m, 1H), 3.42 (dd, J = 12.9, 7.0 Hz, 2H), 1.73–1.61 (m, 2H), 1.01 (t, J = 7.4 Hz, 3H). ^{13}C NMR (101 MHz, $CDCl_3$) δ 165.10, 151.13, 140.84, 133.75, 127.18, 125.76, 125.13, 120.48, 42.35, 22.84, 11.36. HRMS (ESI) *m/z*: 259.0518 (Calcd. for $[M+Na^+]^+$: 259.0517 *m/z*).

4.2.2.2. N-butyl-3-oxobenzo[d]isothiazole-2(3H)-carboxamide ***(2b)***. Compound **2b** was prepared according to standard procedure B by using **1a** and Butylamine, obtained a white solid in 78% yield. ^{1}H NMR (400 MHz, $CDCl_3$) δ 8.88 (s, 1H), 8.02 (d, J = 7.9 Hz, 1H), 7.75–7.65 (m, 1H), 7.58 (d, J = 8.1 Hz, 1H), 7.42 (t, J = 7.5 Hz, 1H), 3.45 (dd, J = 12.8, 7.0 Hz, 2H), 1.63 (dt, J = 19.7, 7.2 Hz, 2H), 1.43 (dq, J = 14.6, 7.3 Hz, 2H), 0.96 (t, J = 7.3 Hz, 3H). ^{13}C NMR (101 MHz, $CDCl_3$) δ 165.10, 151.10, 140.86, 133.75, 127.18, 125.76, 125.15, 120.49, 40.38, 31.58, 20.03, 13.70. HRMS (ESI) *m/z*: 273.0698 (Calcd. for $[M+Na^+]^+$:273.0702 *m/z*).

4.2.2.3. N-(furan-2-ylmethyl)-3-oxobenzo[d]isothiazole-2(3H)-carboxamide ***(2c)***. Compound **2c** was prepared according to standard procedure B by using **1a** and furan-2-ylmethanamine, obtained a white solid in 69% yield. ^{1}H NMR (400 MHz, $CDCl_3$) δ 9.20 (s, 1H), 8.00 (d, J = 7.9 Hz, 1H), 7.74–7.64 (m, 1H), 7.57 (d, J = 8.1 Hz, 1H), 7.47–7.33 (m, 2H), 6.33 (dt, J = 6.1, 2.5 Hz, 2H), 4.63 (d, J = 5.7 Hz, 2H). ^{13}C NMR (101 MHz, $CDCl_3$) δ 165.10, 151.01, 150.53, 142.49, 140.89, 133.90, 127.28, 125.83, 124.88, 120.49, 110.45, 107.86, 37.46. HRMS (ESI) *m/z*: 297.0296 (Calcd. for $[M+Na^+]^+$:297.0304 *m/z*).

4.2.3. Preparation of ebsulfurs Ebs-R following procedure C

To a stirred solution of **1f** (3.0 equiv) in DCM was added DCC (1.3 equiv), DMAP (0.13 equiv) and Rhodamine B (1.0 equiv) at 0 °C. The reaction mixture was stirred for 10 min at 0 °C, and then overnight at room temperature, the solvent was removed in vacuum and extracted with DCM (3 × 10 mL). The combined organic extracts were dried over anhydrous Na_2SO_4, the solvent removed was under reduced pressure, and the crude product was purified by flash column chromatography on silica gel ($CHCl_3/CH_3OH$, 9:1) to afford the final compound **Ebs-R**, as dark purple crystals with metallic glass, yield 50%. ^{1}H NMR (400 MHz, $CDCl_3$) δ 8.38 (dd, J = 7.7, 1.2 Hz, 1H), 8.00 (d, J = 7.8 Hz, 1H), 7.87–7.75 (m, 3H), 7.68–7.62 (m, 1H), 7.41 (t, J = 7.5 Hz, 1H), 7.30 (dd, J = 7.5, 1.1 Hz, 1H), 7.08 (d, J = 9.5 Hz, 2H), 6.92 (dd, J = 9.5, 2.4 Hz, 2H), 6.76 (d, J = 2.4 Hz, 2H), 4.36 (t, J = 5.1 Hz, 2H), 4.12 (t, J = 5.1 Hz, 2H), 3.63 (q, J = 7.1 Hz, 8H), 1.32 (t, J = 7.1 Hz, 12H). ^{13}C NMR (101 MHz, $CDCl_3$) δ 165.58, 164.53, 158.67, 157.67, 155.48, 140.78, 133.87, 133.44, 132.10, 131.67, 131.28, 130.73, 130.26,

129.09, 126.35, 125.52, 123.85, 121.15, 114.32, 113.44, 96.23, 63.74, 46.13, 42.65, 12.67. HRMS (ESI) *m/z*: 620.2569 (Calcd. for $[M-Cl^-]^+$:620.2577 *m/z*).

4.3. Over-expression and purification of NDM-1

NDM-1 was overexpressed and purified as previously described [26]. Truncated wild type NDM-1 (Q37-R270) was cloned into pET-26b vector to facilitate protein folding and purification. The recombinant plasmid was transformed in *E. coli* BL21 (DE3) and expressed with a molecular mass of approximately 25.1 kDa. The cells were plated on LB-agar plates containing 25 μg/mL kanamycin, a single colony was used to inoculate 50 mL of LB containing 25 μg/mL kanamycin. After the preculture grew overnight at 37 °C, 10 mL of overnight culture cells in LB was used to inoculate 4 × 1 L of LB containing 25 μg/mL kanamycin. The cells were allowed to grow at 37 °C with shaking until the cells reached an optical density at 600 nm of 0.6–0.8. Protein production was induced with 1 mM IPTG, and the cells were shaken at 25 °C for 3 h. The cells were collected by centrifugation (30 min at 8275*g*) and re-suspended in 25 mL of 30 mM Tris, pH 8.0, containing 500 mM NaCl. The cells were lysed by ultrasonication, and the cell debris was separated by centrifugation (30 min at 32,583*g*). The cleared supernatant was dialyzed versus 30 mM Tris, pH 8.0, containing 100 μM $ZnCl_2$ for 36 h at 4 °C, centrifuged (25 min at 32,583*g*) to remove insoluble matter, and loaded onto an equilibrated Q-Sepharose column. Bound proteins were eluted with a 0–500 mM NaCl gradient in 30 mM Tris, pH 8.0, containing 100 μM $ZnCl_2$ at 2 mL/min. Fractions (2 mL) containing NDM-1 were pooled and concentrated with an Amicon ultrafiltration cell equipped with an YM-10 membrane. The crude protein NDM-1 was run through a G75 column and eluted with 30 mM Tris, pH 8.0, containing 200 mM NaCl. Protein purity was ascertained by SDS-PAGE and protein concentration was determined using Beer's law and an extinction coefficient of 27,960 $M^{-1}\,cm^{-1}$ at 280 nm.

4.4. Determination of IC_{50} values

The inhibitor concentration causing 50% decrease of enzyme activity (IC_{50}) was determined at 37 °C using cefazolin as substrate of NDM-1. Inhibitors were dissolved in a small volume of DMSO and then diluted with 30 mM Tris, pH 7.5 for NDM-1. The final concentrations of DMSO in inhibition experiments were below 0.1%, control experiments verified that the 0.1% DMSO had no inhibitory activity against the MβLs tested. All inhibitors were assayed at six different concentrations ranging from 0 to 25 μM, and substrate concentration was 50 μM. Enzyme and inhibitor were pre-incubated for 20 h before adding cefazolin. The hydrolysis of cefazolin was monitored at 262 nm on an Agilent UV8453 spectrometer, and the hydrolytic rates were determined in triplicate. The IC_{50} values for all analyzed compounds were calculated by plotting the average percentage inhibition against inhibitor concentration and fitting of the data using GraphPad Prism 5.0 in a logistic dose-response model (see Supporting Information for IC_{50} measurements).

4.5. Equilibrium dialysis

NDM-1 (final concentration 8 μM) in 5 mL of 50 mM HEPES at pH 7.5 was mixed with **1g** at a concentration between 0 and 200 μM. After incubation for 2 h, the solutions were dialyzed versus 500 mL of metal-free 50 mM HEPES at pH 7.5 for 3 × 4 h (dialysis tubing MWCO 8000–14000, Bioreagent). The Zn(II) ion content in the resulting NDM-1 samples was determined using inductively coupled plasma with atomic emission spectroscopy (ICP-AES, IRIS Advantage). A calibration curve with four standards and a correlation coefficient of greater than 0.999 was generated using Zn reference solutions from Fisher Scientific. The emission wavelength was set to 213.856 nm, as previously described [17,26].

4.6. Determination of MIC

Single colony of *E. coli* BL21 (DE3) containing plasmids pET26b-NDM-1 on LB agar plates was transferred to 5 mL of Mueller-Hinton (MH) liquid medium and grown at 37 °C overnight. The bacterial cells were collected by centrifugation (4150*g*, 10 min). After discarding the supernatant, the pelleted cells were re-suspended in MH medium and diluted to an OD_{600} of 0.5. MIC values were determined by using the Clinical and Laboratory Standards Institute (CLSI) macrodilution (tube) broth method [27]. The MIC was interpreted as the lowest concentration of the drug that completely inhibited the visible growth of bacteria after incubating plates for at least 16 h at 37 °C. Each inhibitor was tested in triplicate in at least two independent experiments and the highest MIC value was reported.

4.7. Identification of labelled protein by SDS-PAGE

Equal volumes of NDM-1 and **Ebs-R** were pre-incubated in 10 mM Tris-HCl, pH 7.5, at 25 °C for 2 h. labelled protein was solubilized in 2 × SDS gel loading buffer (100 mM Tris-HCl buffer (pH 6.8), 2.5% SDS, 20% glycerol or 100 mM Tris-HCl buffer (pH 6.8), 2.5% SDS, 20% glycerol and 10% mercaptoethanol) and resolved by SDS-PAGE [34]. The gel was visualized under UV light at 365 nm, and then was stained with Coomassie Brilliant Blue. All images of the gels were captured using an iPhone 6 s.

4.8. Fluorescence imaging and flow cytometer analysis

NDM-1 harbored *E. coli* cells (OD_{600} = 0.5) were incubated with compound **Ebs-R** (0–40 μM) in tubes at 37 °C for different time. After incubation, the cells were repeatedly washed with PBS for five times (10,400*g*, 5 min), to remove any adsorbed **Ebs-R** on surface of the cell. The cells were re-suspended in PBS to give the final samples for confocal microscopic imaging and flow cytometer analysis [20].

4.9. Cytotoxicity assays

A cytotoxicity of inhibitors **1g**, **2a** and **Ebs-R** to mouse fibro-blast cells (L929) was assayed as pervious described [35]. The cells with a density of 1.0×10^4 cells/well in 100 μL of culture medium were seeded into 96-well plates and maintained for 24 h. Then solutions of inhibitors **1g**, **2a** and **Ebs-R** with work concentrations (2.5, 5, 10, 20, 40, and 80 μM) were added to 96-well plates, respectively, and incubated for another 48 h. Six wells containing only cells suspended in a mixture of 99 μL of complete medium and 1 μL of DMSO were used as the control for investigating cell-viability. Three wells containing only the complete medium were used as the blank control. Following that, the medium was removed, and 100 μL of fresh culture medium and 10 μL of CCK8 were added to each well. After incubation for 4 h, the 96-well plates were then vigorously shaken to solubilize the formed product and the absorbance at a wavelength of 490 nm was read on a Microplate Reader and analyzed. All experiments were conducted in triplicate.

Acknowledgments

This work was supported by grants 81361138018 and 21572179 (to K. W. Y.) from the National Natural Science Foundation of China.

Conflicts of interest

None.

Appendix A. Supplementary material

Supplementary data to this article can be found online at https://doi.org/10.1016/j.bioorg.2018.11.035.

References

[1] S.M. Drawz, R.A. Bonomo, Three decades of β-lactamase inhibitors, Clin. Microbiol. Rev. 23 (2010) 160–201.
[2] A.L. Demain, R.P. Elander, The beta-lactam antibiotics: past, present, and future, Antonie Van Leeuwenhoek. 75 (1999) 5–19.
[3] A.A. Medeiros, Evolution and dissemination of beta-lactamases accelerated by generations of beta-lactam antibiotics, Clin. Infect. Dis. 24 (Suppl 1) (1997) S19–S45.
[4] R.P. Ambler, The structure of β-lactamases, Philosop. Trans. R. Soc. Lond.: Series B Biol. Sci. 289 (1980) 321–331.
[5] Z.X. Hu, G. Periyannan, B. Bennett, M.W. Crowder, Role of the Zn1 and Zn2 sites in metallo-beta-lactamase L1, JACS 130 (2008) 14207–14216.
[6] M.W. Crowder, J. Spencer, A.J. Vila, Metallo-beta-lactamases: novel weaponry for antibiotic resistance in bacteria, Acc. Chem. Res. 39 (2006) 721–728.
[7] G. Garau, I. García-Sáez, C. Bebrone, et al., Update of the standard numbering scheme for class B β-lactamases, Antimicrob. Agents Chemother. 48 (2004) 2347–2349.
[8] M.R. Meini, L.I. Llarrull, A.J. Vila, Overcoming differences: the catalytic mechanism of metallo-β-lactamases, FEBS Lett. 589 (2016) 3419–3432.
[9] P.W. Groundwater, S. Xu, F. Lai, et al., New delhi metallo-β-lactamase-1: structure, inhibitors and detection of producers, Future Med. Chem. 8 (2016) 993–1012.
[10] A.U. Khan, L. Maryam, R. Zarrilli, Structure, genetics and worldwide spread of new delhi metallo-β-lactamase (NDM-1): a threat to public health, BMC Microbiol. 17 (2017) 101.
[11] D. Yong, M.A. Toleman, C.G. Giske, et al., Characterization of a new metallo-β-lactamase gene, blandm-1, and a novel erythromycin esterase gene carried on a unique genetic structure in klebsiella pneumoniae sequence type 14 from india, Antimicrob. Agents Chemother. 53 (2009) 5046–5054.
[12] T.R. Walsh, Emerging carbapenemases: a global perspective, Int. J. Antimicrob. Agents 36 (2010) S8–S14.
[13] D.T. King, L.J. Worrall, R. Gruninger, N.C.J. Strynadka, New delhi metallo-β-lactamase: structural insights into β-lactam recognition and inhibition, JACS 134 (2012) 11362–11365.
[14] Y. Guo, J. Wang, G. Niu, et al., A structural view of the antibiotic degradation enzyme NDM-1 from a superbug, Protein Cell 2 (2011) 384.
[15] A.M. King, S.A. Reid-Yu, W.L. Wang, et al., Aspergillomarasmine a overcomes metallo-β-lactamase antibiotic resistance, Nature 510 (2014) 503–506.
[16] L.E. Horsfall, G. Garau, B.M.R. Liénard, et al., Competitive inhibitors of the cpha metallo-β-lactamase from aeromonas hydrophila, Antimicrob. Agents Chemother. 51 (2007) 2136–2142.
[17] A.Y. Chen, P.W. Thomas, A.C. Stewart, et al., Dipicolinic acid derivatives as inhibitors of new delhi metallo-β-lactamase-1, J. Med. Chem. 60 (2017) 7267–7283.
[18] J. Brem, R. Cain, S. Cahill, et al., Structural basis of metallo-β-lactamase, serine-β-lactamase and penicillin-binding protein inhibition by cyclic boronates, Nat. Commun. 7 (2016) 12406.
[19] J. Chiou, S. Wan, K.F. Chan, et al., Ebselen as a potent covalent inhibitor of new delhi metallo-β-lactamase (NDM-1), Chem. Commun. 51 (2015) 9543–9546.
[20] C. Chen, Y. Xiang, K.W. Yang, et al., A protein structure-guided covalent scaffold selectively targets the B1 and B2 subclass metallo-β-lactamases, Chem. Commun. 54 (2018) 4802–4805.
[21] H.M. Zhang, Q. Hao, Crystal structure of NDM-1 reveals a common β-lactam hydrolysis mechanism, Faseb J. Off. Publ. Feder. Am. Soc. Experim. Biol. 25 (2011) 2574–2582.
[22] J. Lu, S.K. Vodnala, A.L. Gustavsson, et al., Ebsulfur is a benzisothiazolone cytocidal inhibitor targeting the trypanothione reductase of trypanosoma brucei, J. Biol. Chem. 288 (2013) 27456–27468.
[23] H.M. Gordhan, S.L. Patrick, M.I. Swasy, et al., Evaluation of substituted ebselen derivatives as potential trypanocidal agents, Biorg. Med. Chem. Lett. 27 (2016) 537–541.
[24] D. Liu, Z. Tian, Z. Yan, et al., Design, synthesis and evaluation of 1,2-benzisothiazol-3-one derivatives as potent caspase-3 inhibitors, Biorg. Med. Chem. 21 (2013) 2960–2967.
[25] H.X. Ngo, S.K. Shrestha, K.D. Green, S. Garneau-Tsodikova, Development of ebsulfur analogues as potent antibacterials against methicillin-resistant staphylococcus aureus, Biorg. Med. Chem. 24 (2016) 6298–6306.
[26] H. Yang, M. Aitha, A.M. Hetrick, et al., Mechanistic and spectroscopic studies of metallo-β-lactamase NDM-1, Biochemistry 51 (2012) 3839–3847.
[27] F.R. Cockerill, Methods for dilution antimicrobial susceptibility tests for bacteria that grow aerobically: approved standard, Clin. Laborat. Standards Instit. (2000).
[28] K.W. Yang, Y. Zhou, Y. Ge, Y. Zhang, Real-time activity monitoring of new delhi metallo-β-lactamase-1 in living bacterial cells by uv-vis spectroscopy, Chem. Commun. 53 (2017) 8014–8017.
[29] S. Mizukami, S. Watanabe, Y. Hori, K. Kikuchi, Covalent protein labeling based on noncatalytic β-lactamase and a designed fret substrate, JACS 131 (2009) 5016–5017.
[30] M. Singha, S. Roy, S.D. Pandey, et al., Use of azidonaphthalimide carboxylic acids as fluorescent templates with a built-in photoreactive group and a flexible linker simplifies protein labeling studies: applications in selective tagging of hcaii and penicillin binding proteins, Chem. Commun. 53 (2017) 13015–13018.
[31] J.M. Xiao, L. Feng, L.S. Zhou, et al., Novel fluorescent cephalosporins: synthesis, antimicrobial activity and photodynamic inactivation of antibiotic resistant bacteria, Eur. J. Med. Chem. 59 (2013) 150–159.
[32] A. Rokney, M. Shagan, M. Kessel, et al., *E. Coli* transports aggregated proteins to the poles by a specific and energy-dependent process, J. Mol. Biol. 392 (2009) 589–601.
[33] X. Yong, J.G. Wilkes, T.J. Moskal, et al., Development of a flow cytometry-based method for rapid detection of escherichia coli and shigella spp. Using an oligonucleotide probe, PLoS One 11 (2016) e0150038.
[34] U.K. Laemmli, Cleavage of structural proteins during the assembly of the head of bacteriophage t4, Nature 227 (1970) 680–685.
[35] D. Gao, A. Li, L. Guan, et al., Solvent-dependent ratiometric fluorescent merocyanine dyes: spectral properties, interaction with bsa as well as biological applications, Dyes Pigm. 129 (2016) 163–173.